"Widening the Roof": Synthesis and Characterization of New Chiral C_1-Symmetric Octahydrofluorenyl Organolanthanide Catalysts and Their Implementation in the Stereoselective Cyclizations of Aminoalkenes and Phosphinoalkenes

Michael R. Douglass, Masamichi Ogasawara, Sukwon Hong, Matthew V. Metz, and Tobin J. Marks*

Department of Chemistry, Northwestern University, Evanston, Illinois 60208-3113

Received May 16, 2001

New chiral C_1-symmetric organolanthanide catalysts of the type $Me_2Si(OHF)(CpR^*)LnN(TMS)_2$ (OHF = η^5-octahydrofluorenyl; Cp = η^5-C_5H_3; R* = (−)-menthyl; Ln = Sm, Y, Lu; TMS = $SiMe_3$) have been synthesized, characterized, and implemented in the enantioselective and diastereoselective cyclizations of aminoalkenes and phosphinoalkenes. $Me_2Si(OHF)(CpR^*)LnCl_2^-Li(DME)_2^+$ catalyst precursors can be prepared in up to ∼90% diastereomeric purity and then converted into the corresponding amido catalysts, which can be isolated in ∼100% diastereomeric purity after recrystallization. The catalyst (*S*)-$Me_2Si(OHF)(CpR^*)YN(TMS)_2$ has been crystallographically characterized. The activity of these catalysts for the hydroamination/cyclization of aminoalkenes and for the hydrophosphination/cyclization of phosphinoalkenes is described. Enantioselectivites as high as 67% are obtained in hydroamination, and diastereoselectivities of as high as 96% are obtained in hydrophosphination.

Introduction

The efficient stereoselective synthesis of chiral molecules represents an ongoing challenge in catalytic chemistry.[1] Organolanthanide complexes[2] have been demonstrated to exhibit unique reactivity and selectivity for chemo-, regio-, and enantioselective hydrogenation of olefins, alkynes, and imines,[3] hydrosilylation of olefins and alkynes,[4] hydroboration of olefins,[5] and various types of polymerization and copolymerization,[6] as well as hydroamination[7,8] and hydrophosphination[9] of several classes of unsaturated organic molecules. To extend further the usefulness of these 4f complexes, there has been a growing effort to develop chiral organolanthanide catalysts for performing useful asymmetric transformations.[10] Modification of *ansa*-lanthanocene frameworks

(1) (a) *Acc. Chem. Res.* **2000**, *6*, 323−440 (Special Asymmetric Catalysis Issue). (b) *Catalytic Asymmetric Synthesis*; Ojima, I., Ed.; VCH: New York, 2000. (c) *Comprehensive Asymmetric Catalysis*; Jacobsen, E. N., Pfaltz, A., Yamamoto, H., Eds.; Springer: Berlin, 1999; Vol. I−III. (d) Noyori, R. *Asymmetric Catalysis in Organic Synthesis*; Wiley: New York, 1994. (e) Blaser, H.-U.; Pugin, B.; Spindler, F. In *Applied Homogeneous Catalysis with Organometallic Compounds*; Cornils, B., Hermann, W. A., Eds.; VCH: Weinheim, Germany, 1996; Vol. 2, pp 992−1009.

(2) For reviews of organolanthanide chemistry, see: (a) Molander, G. A. *Chemtracts: Org. Chem.* **1998**, *18*, 237−263. (b) Edelmann, F. T. *Top. Curr. Chem.* **1996**, *179*, 247−276. (c) Edelmann, F. T. in *Comprehensive Organometallic Chemistry*; Wilkinson, G., Stone, F. G. A., Abel, E. W., Eds.; Pergamon Press: Oxford, U.K., 1995; Vol. 4, Chapter 2. (d) Schumann, H.; Meese-Marktscheffel, J. A.; Esser, L. *Chem. Rev.* **1995**, *95*, 865−986. (e) Schaverien, C. J. *Adv. Organomet. Chem.* **1994**, *36*, 283−362. (f) Evans, W. J. *Adv. Organomet. Chem.* **1985**, *24*, 131−177. (g) Marks, T. J.; Ernst, R. D. In *Comprehensive Organometallic Chemistry*; Wilkinson, G., Stone, F. G. A., Abel, E. W., Eds.; Pergamon Press: Oxford, U.K., 1982; Chapter 21.

(3) Hydrogenation: (a) Obora, Y.; Ohta, T.; Stern, C. L.; Marks, T. J. *J. Am. Chem. Soc.* **1997**, *119*, 3745−3755. (b) Roesky, P. W.; Denninger, U.; Stern, C. L.; Marks, T. J. *Organometallics* **1997**, *16*, 4486-4492. (c) Haar, C. M.; Stern, C. L.; Marks, T. J. *Organometallics* **1996**, *15*, 1765−1784. (d) Jeske, G.; Lauke, H.; Mauermann, H.; Swepston, P. N.; Schumann, H.; Marks, T. J. *J. Am. Chem. Soc.* **1985**, *107*, 8091−8103.

(4) Hydrosilylation: (a) Molander, G. A.; Corvette, C. P. *Organometallics* **1998**, *17*, 5504−5512. (b) Schumann, H.; Keitsch, M. R.; Winterfeld, J.; Muhle, S.; Molander, G. A. *J. Organomet. Chem.* **1998**, *559*, 181−190. (c) Fu, P.-F.; Brard, L.; Li, Y.; Marks, T. J. *J. Am. Chem. Soc.* **1995**, *117*, 7157−7168. (d) Molander, G. A.; Julius, M. *J. Org. Chem.* **1992**, *57*, 6347−6351. (e) Sakakura, T.; Lautenschlager, H.; Tanaka, M. *J. Chem. Soc., Chem. Commun.* **1991**, 40−41.

(5) Hydroboration: (a) Molander, G. A.; Pfeiffer, D. *Org. Lett.* **2001**, *3*, 361−363. (b) Bijpost, E. A.; Duchateau, R.; Teuben, J. H. *J. Mol. Catal.* **1995**, *95*, 121−128. (c) Harrison, K. N.; Marks, T. J. *J. Am. Chem. Soc.* **1992**, *114*, 9220−9221.

(6) Polymerization: (a) Koo, K.; Fu, P.-F.; Marks, T. J. *Macromolecules* **1999**, *32*, 981−988. (b) Giardello, M. A.; Yamamoto, Y.; Brard, L.; Marks, T. J. *J. Am. Chem. Soc.* **1995**, *117*, 3276−3277. (c) Reference 3d. (d) Watson, P. L. *J. Am. Chem. Soc.* **1982**, *104*, 337−339.

(7) (a) Gilbert, A. T.; Davis, B. L.; Emge, T. J.; Broene, R. D. *Organometallics* **1999**, *18*, 2125−2132. (b) Molander, G. A.; Dowdy, E. D. *J. Org. Chem.* **1999**, *64*, 6515−6517. (c) Molander, G. A.; Dowdy, E. D. *J. Org. Chem.* **1998**, *63*, 8983−8988.

(8) Aminoalkenes: (a) Ryu, J.-S.; Marks, T. J.; McDonald, F. E. *Abstracts of Papers*, 221st National Meeting of the American Chemical Society, San Diego, CA, April 1−5, 2001; American Chemical Society: Washington, DC, 2001; abstract ORGN 265; *Org. Lett.* **2001**, *3*, 3091−3094. (b) Gagné, M. R.; Stern, C. L.; Marks, T. J. *J. Am. Chem. Soc.* **1992**, *114*, 275−294. (c) Gagné, M. R.; Marks, T. J. *J. Am. Chem. Soc.* **1989**, *111*, 4108−4109. Aminoalkynes: (d) Li, Y.; Marks, T. J. *J. Am. Chem. Soc.* **1998**, *120*, 1757−1771. (e) Li, Y.; Marks, T. J. *J. Am. Chem. Soc.* **1996**, *118*, 9295−9306. (f) Li, Y.; Marks, T. J. *Organometallics* **1996**, *15*, 3370−3372. (g) Li, Y.; Marks, T. J. *J. Am. Chem. Soc.* **1996**, *118*, 707−708. (h) Li, Y.; Fu, P.-F.; Marks, T. J. *Organometallics* **1994**, *13*, 439−440. Aminoallenes: (i) Arredondo, V. M.; McDonald, F. E.; Marks, T. J. *Organometallics* **1999**, *10*, 1949−1960. (j) Arredondo, V. M.; Tian, S.; McDonald, F. M.; Marks, T. J. *J. Am. Chem. Soc.* **1999**, *121*, 3633−3639. (k) Arredondo, V. A.; McDonald, F. M.; Marks, T. J. *J. Am. Chem. Soc.* **1998**, *120*, 4871−4872. Aminodienes: (l) Hong, S.; Marks, T. J. *Abstracts of Papers*, 221st National Meeting of the American Chemical Society, San Diego, CA, April 1−5, 2001; American Chemical Society: Washington, DC, 2001; abstract INOR 613.

(9) (a) Douglass, M. R.; Stern, C. L.; Marks, T. J. *J. Am. Chem. Soc.* **2001**, *123*, 10221−10238. (b) Douglass, M. R.; Marks, T. J. *J. Am. Chem. Soc.* **2000**, *122*, 1824−1825.

10.1021/om0104013 CCC: $22.00
Publication on Web 12/19/2001

by appending chiral substituents to create C_1-symmetric complexes of the type $Me_2Si(Cp'')(CpR^*)LnE(TMS)_2$ ($Cp'' = \eta^5$-Me_4C_5; $Cp = \eta^5$-C_5H_3; Ln = La, Sm, Y, Lu; R* = (+)-neomenthyl, (−)-menthyl; E = N, CH; TMS = $SiMe_3$; **A**, **B**) is one approach that has been investi-

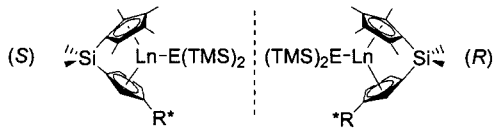

A **B**

gated.[11] This strategy addresses three goals: (i) it preserves lanthanocene stereoelectronic characteristics which promote high reactivity; (ii) the metallocene ligand structure imparts high stability and solubility; (iii) in synthesis, the diastereomeric products can in principle be readily separated. In addition, C_1-symmetric catalysts have an inherent advantage over other more highly symmetric catalysts (e.g., C_2-symmetric) in that even if diastereomers undergo racemization, the equilibrium diastereomeric ratio is rarely near 1:1 and thus, high catalyst diastereopurity can still be maintained.[12] The results to date for enantioselective transformations with catalysts of type **A** and **B** have been promising. Thus, olefin hydrogenation (up to 96% ee),[11] hydrosilylation (up to 68% ee),[4c] and isospecific methyl methacrylate polymerization (*mm* up to 94%)[6b] are effected with good chemo- and regioselectivity. Although an epimerization process in the presence of protic donor amines is observed to convert configurationally pure catalysts into mixtures of diastereomers, equilibrium ratios are typically far from 1:1, and good selectivities for intramolecular hydroamination/cyclization of aminoalkenes are also observed (up to 74% ee; >95% de).[13]

These results with first-generation chiral C_1-symmetric organolanthanides led us to question whether it might be possible to increase top−bottom ligand−substrate steric discrimination by increasing the "wingspan" of the upper ligand, thereby increasing the selectivity of the cyclizations. Specifically, we undertook to introduce the stereodemanding, electron-donating octahydrofluorenyl (OHF) ligand which, when linked to a smaller Cp−R* group, would lead to a new class of C_1-symmetric organolanthanide catalysts that could potentially provide increased enantiofacial discrimination in prochiral substrate recognition/activation. Thus, OHF complexes of structure **C** should impart significantly greater steric tranverse discriminatory demands than the Cp″ analogue **D**,[14] and although we previously demonstrated that analogous C_1-symmetric group 4

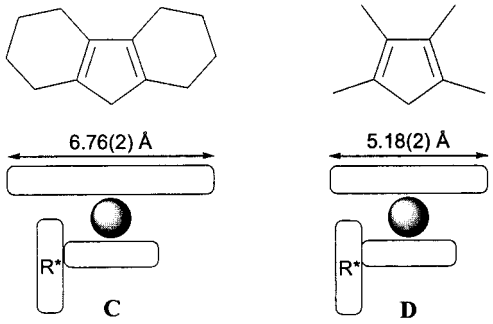

C **D**

OHF-based catalysts[14] are more effective in isospecific propylene polymerization than **D**-type catalysts,[15] this ligand has not yet been applied in asymmetric organolanthanide catalysis.[16] We report here the synthesis, characterization, and molecular structures of new chiral OHF organolanthanide catalysts of the class $Me_2Si(OHF)(CpR^*)LnN(TMS)_2$ and an investigation of their catalytic properties for the intramolecular enantio- and diastereoselective cyclizations of amino- and phosphinoalkenes.

Experimental Section

Materials and Methods. All manipulations of air-sensitive materials were carried out with rigorous exclusion of oxygen and moisture in flame- or oven-dried Schlenk-type glassware on a dual-manifold Schlenk line, or interfaced to a high-vacuum line (10^{-6} Torr), or in a nitrogen-filled Vacuum Atmospheres glovebox with a high-capacity recirculator (<1 ppm of O_2). Argon (Matheson, prepurified) was purified by passage through a MnO oxygen-removal column and a Davison 4A molecular sieve column. Solvents used for catalyst synthesis and catalytic reactions were dried over Na/K alloy, stored under high vacuum, and vacuum-transferred into reaction vessels immediately prior to use. Deuterated solvents were purchased from Cambridge Isotope Laboratories. Benzene-d_6 and toluene-d_6 (Cambridge Laboratories; all 99+ atom % D) used for NMR-scale reactions and kinetic measurements were stored in vacuo over Na/K alloy in resealable bulbs, and were vacuum-transferred immediately prior to use. All organic starting materials were purchased from Aldrich Chemical Co., Farchan Laboratories Inc., or Lancaster Synthesis Inc., and were used without further purification unless otherwise stated. Me_3SiCH_2Li and $(TMS)_2NK$ were purified by sublimation prior to use. Anhydrous YCl_3, $SmCl_3$, and $LuCl_3$ were purchased from Aldrich Chemical Co. and used as received. Substrates **5**, **7**, **9**, **11**, **13**, and **15** were prepared as reported previously,[8,9] dried a minimum of two times as solutions in benzene-d_6 or toluene-d_6 over freshly activated Davison 4A molecular sieves, and degassed by freeze−pump−thaw methods. They were then stored in vacuum-tight storage flasks. Solutions of **13** and **15** were protected from light to minimize noncatalytic endocyclization reactions.[9]

Physical and Analytical Measurements. NMR spectra were recorded on a Varian Gemini-300 (FT, 300 MHz, ^{1}H; 75 MHz, ^{13}C), Mercury-400 (FT, 400 MHz, ^{1}H; 100 MHz, ^{13}C; 162 MHz, ^{31}P), or Inova-500 (FT, 500 MHz, ^{1}H; 125 MHz, ^{13}C; 202

(10) (a) Muci, A. R.; Bercaw, J. E. *Tetrahedron Lett.* **2000**, *41*, 7609−7612. (b) Yoder, J. C.; Day, M. W.; Bercaw, J. E. *Organometallics* **1998**, *17*, 4946−4958. (c) Hultzch, K. C.; Spaniol, T. P.; Okuda, J. *Organometallics* **1997**, *16*, 4845−4856. (d) Hultzch, K. C.; Okuda, J. *Macromol. Rapid Commun.* **1997**, *18*, 809−815. (e) Yasuda, H.; Ihara, E. *Macromol. Chem. Phys.* **1995**, *196*, 2417−2441. (f) Coughlin, E. B.; Bercaw, J. E. *J. Am. Chem. Soc.* **1992**, *114*, 7607−7607.

(11) Giardello, M. A.; Conticello, V. P.; Brard, L.; Sabat, M.; Rheingold, A. L.; Stern, C.; Marks, T. J. *J. Am. Chem. Soc.* **1994**, *116*, 10212−10240.

(12) For a discussion of some of the attractions of nonsymmetric versus C_2 ligation, see: Helmchen, G.; Pfaltz, A. *Acc. Chem. Res.* **2000**, *33*, 336−345.

(13) Giardello, M. A.; Conticello, V. P.; Brard, L.; Gagné, M. R.; Marks, T. J. *J. Am. Chem. Soc.* **1994**, *116*, 10241−10254.

(14) Obora, Y.; Stern, C. L.; Marks, T. J.; Nickias, P. N. *Organometallics* **1997**, *16*, 2503−2505.

(15) For other group 4 applications of fluorenyl ligands in olefin polymerization, see: (a) Schellenberg, J. *J. Polym. Sci., Polym. Chem.* **2000**, *38*, 2428−2439. (b) Leino, R.; Luttikhedde, H. J. G.; Lehtonen, A.; Wilen, C. E.; Nasman, J. H. *J. Organomet. Chem.* **1997**, *546*, 219−224. (c) Jany, G.; Fawzi, R.; Steimann, M.; Rieger, B. *Organometallics* **1997**, *26*, 554−550. (d) Rieger, B.; Jany, G. *Chem. Ber.* **1994**, *127*, 2417−2419.

(16) For examples of organolanthanides with fluorenyl ligands, see: (a) Qian, C.; Nie, W.; Sun, J. *Organometallics* **2000**, *19*, 4134−4140. (b) Lee, M. H.; Hwang, J.-W.; Kim, Y.; Kim, J.; Han, Y.; Do, Y. *Organometallics* **1999**, *18*, 5124−5129.

MHz, ^{31}P) instrument. Chemical shifts (δ) for ^{1}H and ^{13}C are referenced to internal solvent resonances and reported relative to $SiMe_4$. Chemical shifts for ^{31}P are reported relative to an external 85% H_3PO_4 standard. NMR experiments on air-sensitive samples were conducted in Teflon-valve-sealed tubes (J. Young). Elemental analyses were carried out by Midwest Microlabs, Indianapolis, IN.

Synthesis of $Me_2Si(OHF)(CpR^*)YCl_2Li(DME)_2$ (3b). The neutral ligand (**1**; 1.00 g, 2.30 mmol) and $TMSCH_2Li$ (435 mg, 4.62 mmol) were placed in a reaction flask in the glovebox, and pentane (ca. 30 mL) was vacuum-transferred into the flask on a high-vacuum line. The mixture was stirred overnight at room temperature to afford a yellow-brown, almost clear suspension. All volatiles were then removed under high vacuum, and YCl_3 (460 mg, 2.36 mmol) was added to the residue in the glovebox. DME (ca. 30 mL) was transferred to the flask on a high-vacuum line, and the suspension was stirred at room temperature for 3 days to yield a clear brown solution. The solution was next evaporated to dryness, and the residue was extracted with ether (3 × 15 mL). The combined ether extracts were filtered and then evaporated to dryness under high vacuum to give a light brown solid. The crude product was recrystallized from hot DME (slow cooling from reflux to room temperature) to afford two crops of the title compound as colorless prisms. Yield: 1.24 g (1.59 mmol, 67%). This material was slightly contaminated by the second diastereomer (~10% by ^{1}H NMR) and could not be purified further by recrystallization; therefore, the diastereomeric mixture was used for the next step without further purification. ^{1}H NMR (500 MHz, THF-d_8): δ 6.12 (s, 1H), 5.58 (s, 1H), 5.48 (s, 1H), 3.42 (s, 8H), 3.26 (s, 12H), 2.53 (m, 8H), 2.19 (m, 3H), 1.99−1.81 (m, 3H), 1.63 (m, 3H), 1.43 (m, 3H), 1.34 (m, 3H), 1.11 (m, 3H), 0.86 (d, 6.5 Hz, 3H), 0.77 (d, 6.5 Hz, 3H) 0.69 (d, 7 Hz, 3H), 0.57 (d, 11.0 Hz, 6H) (minor isomer: Cp resonances δ 5.61 (d, 2H), 6.06 (t, 1H)). Anal. Calcd for $C_{38}H_{64}O_4Cl_2LiSiY$: C, 58.53; H, 8.27. Found: C, 58.24; H, 8.40.

Synthesis of $Me_2Si(OHF)(CpR^*)SmCl_2Li(DME)_2$ (3a). This samarium complex was isolated as yellow prisms by a procedure analogous to that described for **3b**, starting from the neutral ligand **1** (3.00 g, 6.90 mmol), Me_3SiCH_2Li (1.32 g, 14.0 mmol), and $SmCl_3$ (1.78 g, 6.93 mmol). Yield: 3.36 g (3.99 mmol, 58%). This product also contains two diastereomers (~9:1 molar ratio by ^{1}H NMR). ^{1}H NMR (500 MHz, THF-d_8; chemical shifts of this complex exhibit a slight concentration dependence; this spectrum was recorded with 8.7 mg of **3a** in 0.7 mL of THF-d_8): δ 11.44 (s, 1H), 6.82 (s, 1H), 6.79 (s, 1H), 4.10 (s, 1H), 3.89 (br q, 11 Hz, 1H), 3.42 (s, 8H), 3.26 (s, 12H), 3.02 (m, 1H), 2.68 (m, 1H), 2.54 (t, 1H), 2.42 (m, 1H), 2.23 (m, 3H), 2.10 (d, 1H), 1.92 (m, 2H), 1.64 (m, 1H), 1.56 (d, 6.5 Hz, 3H), 1.47 (m, 3H), 1.26 (q, 1H), 1.14 (s, 3H), 1.02 (d, 6.5 Hz, 4H), 0.85 (br s, 2H), 0.73 (br s, 1H), 0.46 (s, 6H), 0.10 (br s, 1H), −0.76 (s, 1H), −1.66 (s, 1H), −2.07 (d, 14.0 Hz, 1H), −3.97 (s, 1H) (minor isomer: Cp resonances: δ 14.30 (br, 1H), 6.03 (br, 1H), 5.04 (br, 1H)). Anal. Calcd for $C_{38}H_{64}O_4Cl_2LiSiSm$: C, 54.26; H, 7.67. Found: C, 54.37; H, 7.87.

Synthesis of $Me_2Si(OHF)(CpR^*)LuCl_2Li(DME)_2$ (3c). This lutetium complex was isolated as colorless prisms by a procedure analogous to that described for **3b**, starting from the neutral ligand **1** (2.50 g, 5.75 mmol), Me_3SiCH_2Li (1.10 g, 11.7 mmol), and $LuCl_3$ (1.62 g, 5.76 mmol). Yield: 3.09 g (3.57 mmol, 62%). This product also contains two diastereomers (~9:1 molar ratio by ^{1}H NMR). ^{1}H NMR (500 MHz, THF-d_8): major isomer δ 6.10 (s, 1H), 5.52 (s, 1H), 5.41 (s, 1H), 3.42 (s, 8H), 3.26 (s, 12H), 2.54 (m, 8H), 2.19 (m, 3H), 1.97−1.80 (m, 3H), 1.60 (m, 3H), 1.41 (m, 3H), 1.31 (m, 3H), 1.08 (qu, 11 Hz, 3H), 0.86 (d, 6.0 Hz, 3H), 0.78 (d, 7.0 Hz, 3H), 0.69 (d, 6.5 Hz, 3H), 0.56 (d, 11.5 Hz, 6H) (minor isomer: Cp resonances δ 6.01 (t, 1H), 5.57 (d, 2H)). Anal. Calcd for $C_{38}H_{64}O_4Cl_2LiLuSi$: C, 52.71; H, 7.45. Found: C, 52.80; H, 7.68.

Synthesis of $Me_2Si(OHF)(CpR^*)YN(TMS)_2$ (4b). $Me_2Si(OHF)(CpR^*)YCl_2Li(DME)_2$ (**3b**; 1.50 g, 1.92 mmol) and $(TMS)_2NK$ (420 mg, 2.00 mmol) were placed in a reaction flask in the glovebox, and then on a high-vacuum line toluene (ca. 30 mL) was vacuum-transferred into the flask. The suspension was stirred at 0 °C for 12 h, and then the volatiles were removed under high vacuum. Pentane (ca. 20 mL) was vacuum-transferred onto the residue, and the resulting suspension was stirred at room temperature with further precipitation of inorganic salts (KCl and LiCl). The suspension was next filtered through a pad of Celite (the Celite pad *must* be dried and degassed under high vacuum at least overnight), and the residue was further extracted with pentane (3 × 20 mL). The combined pentane filtrates were then evaporated to dryness, and the residue was recrystallized from hot hexane to afford two crops of the title complex as diastereomerically pure, colorless crystals. Yield: 1.05 g (1.54 mmol, 80%). ^{1}H NMR (400 MHz, C_6D_6): δ 6.51 (t, 1H), 5.92 (t, 1H), 5.77 (t, 1H), 2.68 (m, 3H), 2.27−2.55 (m, 7H), 1.32−1.85 (m, 12H), 1.14 (d, 6.4 Hz, 3H), 0.84−1.08 (m, 4H), 0.87 (d, 7.2 Hz, 3H), 0.78 (s, 3H), 0.71 (s, 3H), 0.69 (d, 7.2 Hz, 3H), 0.23 (s, 9H), 0.17 (s, 9H). ^{13}C NMR (125 MHz, C_6D_6): δ 140.8, 127,8, 125.7 (d, 17 Hz), 118.6, 116.7, 115.9, 114.1, 109.8, 52.5, 41.9, 41.8, 36.4, 33.8, 27.5, 27.4, 27.0, 25.6, 24.8, 24.6, 24.3, 24.2, 23.9, 23.8, 23.2, 22.2, 16.2, 5.1, 4.2. Anal. Calcd for $C_{36}H_{62}NSi_3Y$: C, 63.40; H, 9.16; N, 2.05. Found: C, 63.10; H, 9.22; N, 2.35.

Synthesis of $Me_2Si(OHF)(CpR^*)SmN(TMS)_2$ (4a). This complex was synthesized as diastereomerically pure, orange prisms from $Me_2Si(OHF)(CpR^*)SmCl_2Li(DME)_2$ (**3a**; 1.50 g, 1.78 mmol) and $(TMS)_2NK$ (390 mg, 1.88 mmol) in toluene in a manner analogous to that described above for **4b**. Yield: 914 mg (1.23 mmol, 69%). ^{1}H NMR (500 MHz, C_6D_6): δ 15.87 (s, 1H), 9.55 (d, 10.5 Hz, 1H), 8.14 (s, 1H), 6.51 (s, 1H), 4.48 (t, 6.0 Hz, 1H), 4.05 (s, 1H), 3.79 (s, 2H), 2.96 (s, 1H), 2.83 (s, 1H), 2.57 (s, 3H), 2.47 (d, 6.0 Hz, 3H), 2.40 (d, 9.5 Hz, 1H), 2.30 (m, 2H), 2.20 (d, 12.0 Hz, 1H), 2.08 (br s, 2H), 1.68 (s, 2H), 1.57 (m, 3H), 1.23 (m, 1H), 0.83 (m, 2H), 0.39 (d, 7.0 Hz, 3H), 0.29 (s, 3H), 0.09 (s, 2H), −2.03 (d, 64.5 Hz, 2H), −4.35 (d, 59.5 Hz, 2H), −5.51 (s, 9H), −6.63 (br, 9H), −8.64 (s, 1H), −13.16 (s, 1H). Anal. Calcd for $C_{36}H_{62}NSi_3Sm$: C, 58.16; H, 8.41; N, 1.88. Found: C, 57.84; H, 8.54; N, 2.09.

Synthesis of $Me_2Si(OHF)(CpR^*)LuN(TMS)_2$ (4c). This complex was synthesized as diastereomerically pure, colorless microcrystals from $Me_2Si(OHF)(CpR^*)LuCl_2Li(DME)_2$ (**3c**; 1.50 g, 1.73 mmol) and $(TMS)_2NK$ (380 mg, 1.83 mmol) in toluene in a manner analogous to that described above for **4b**. Yield: 962 mg (1.25 mmol, 72%). ^{1}H NMR (500 MHz, C_6D_6): δ 6.58 (s, 1H), 5.89 (t, 2.5 Hz, 1H), 5.72 (s, 1H), 2.68 (m, 3H), 2.35−2.56 (m, 7H), 1.35−1.79 (m, 12H), 1.12 (d, 6.0 Hz, 3H), 1.01 (m, 4H), 0.86 (d, 7.0 Hz, 3H), 0.79 (s, 3H), 0.70 (d, 8.5 Hz, 6H), 0.25 (s, 9H), 0.19 (s, 9H). ^{13}C NMR (125 MHz, C_6D_6): δ 139.9, 127.2, 123.9 (d, 11 Hz), 118.9, 117.3, 114.3, 112.2, 110.4, 52.4, 41.7, 41.7, 36.4, 33.8, 27.6, 27.5, 27.0, 25.6, 24.7, 24.5, 24.4, 24.0, 23.7, 23.2, 22.1, 16.3, 5.7, 4.0, 0.1, −0.6. Anal. Calcd for $C_{36}H_{62}LuNSi_3$: C, 56.29; H, 8.14; N, 1.82. Found: C, 56.20; H, 7.99; N, 1.86.

Typical NMR-Scale Catalytic Reactions. In the glovebox, the organolanthanide precatalyst (2−3 mg) was weighed into an NMR tube equipped with a Teflon valve, and C_6H_6 (0.1 mL) along with ~10 equiv *n*-propylamine was added to activate the catalyst. After 30 min, the solvent was removed in vacuo and C_6D_6 (~0.5 mL) was added. On the high-vacuum line, the tube was evacuated while the benzene solution was frozen at −78 °C, and then the substrate (ca. 1.0 M in C_6D_6, 0.2−0.3 mL, 30−150-fold molar excess) was added either via syringe under an Ar flush (aminoalkenes) or by vacuum-transfer (phosphinoalkenes). The tube was evacuated and back-filled with Ar three times while frozen at −78 °C, and then the tube was sealed, thawed, and brought to the desired temperature; the ensuing reaction was monitored by ^{1}H NMR (and ^{31}P NMR when applicable). All products are known compounds.

Determination of Product Stereochemical Configuration. After consumption of substrate was complete as

Table 1. Summary of the Crystal Structure Data for $Me_2Si(OHF)(CpR^*)YN(TMS)_2$ (4b)

formula	$C_{36}H_{62}NSi_3Y$
cryst syst	orthorhombic
space group	$P2_12_12_1$
a	9.7969(8) Å
b	19.075(2) Å
c	20.090(3) Å
V	3754.3(8) Å^3
Z	4
d_{calcd}	1.207 g/cm^3
cryst size, mm	0.24 × 0.19 × 0.12
color, habit	colorless, block
diffractometer	Bruker SMART-1000 CCD
temp	−120 °C
μ	1.673 mm^{-1}
transmission factors, range	0.66068−0.83479
radiation	Mo Kα (λ = 0.710 69 Å)
exposure time	15 s
scan width	0.30°
θ range	1.47° to 29.29°
intensities (unique, R_i)	34 718 (9030, 0.0353)
intensities > 3σ	34 718
no. of params	370
R1	0.0249
wR2 ($[\sum(w(F_o^2 - F_c^2)^2)/[\sum(w(F_o^2)^2]]^{1/2}$)	0.0560
min, max density in ΔF map	−0.180, 0.387 e/Å^3

assayed by ^{1}H NMR, the reaction solution was separated from the catalyst residue by vacuum transfer. The enantioselectivity of the hydroamination reactions was assayed by Mosher amide analysis[17] using GC. The optical rotation values of the amines were determined by diluting the solution to a total volume of 1.5 mL of C_6D_6 and measuring the optical rotation of the sample with a polarimeter. The concentrations of the solutions were as follows: **6**, 0.0304 g/mL; **8**, 0.00959 g/mL; **10**, 0.0148 g/mL; **12**, 0.0111 g/mL. For **6** and **8**, the correlation between optical rotation and absolute configuration has been established.[18] The diastereoselectivity of the hydrophosphination reactions was determined by ^{31}P NMR spectroscopy of the known products immediately upon completion of the reaction, with ^{31}P NMR chemical shift assignments for the various *cis* and *trans* isomers having already been established.[9,19]

X-ray Crystallographic Study of (*S*)-$Me_2Si(OHF)(CpR^*)YN(TMS)_2$ (4b). A suitable crystal of **4b** was mounted using oil (Infineum V 8512) on a glass fiber and transferred to a Bruker SMART-1000 CCD diffractometer. Crystal data collection parameters are summarized in Table 1. Lattice parameters were determined from 25 scans, and cell reduction calculations on all data showed **4b** to crystallize in the orthorhombic space group $P2_12_12_1$.[20] Intensity data were corrected for Lorentz, polarization, and anomalous dispersion effects.[20] The structure was solved using direct methods[21] and expanded using Fourier techniques.[22] The final cycle of full-matrix least-squares refinement[23] was based on 9030 observed reflections (I > 2.00σ(*I*)) and 370 variable parameters, and converged (largest parameter shifts were 0.001 times the esd) with unweighted and weighted agreement factors of R1 = 0.0249 and wR2 = 0.0560. Hydrogen atoms were included but not refined. The largest and smallest peaks in the final difference map were −0.180 and 0.387 e/Å^3, respectively. The structure was confirmed to be the *S* isomer because (1) refinement as the *R* isomer led to a higher *R* value, and (2) it had the appropriate Flack parameter, representing the anomalous dispersion.

Scheme 1. Ligand and Catalyst Synthesis

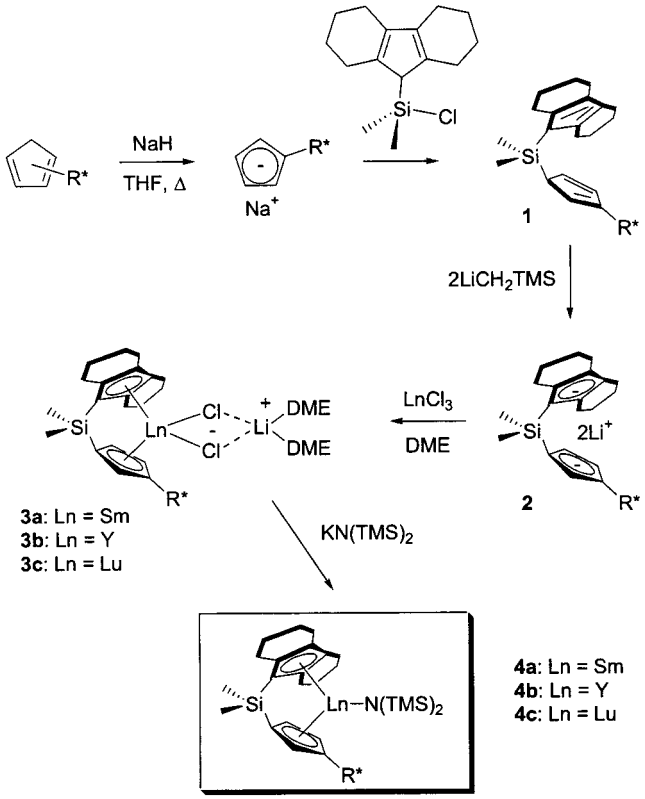

Results and Discussion

Synthesis of Precatalysts. The neutral ligand precursor $Me_2Si(OHF\text{-}H)(CpR^*\text{-}H)$ (**1**) was synthesized according to our published procedure (Scheme 1).[14] Since the ligand dilithio salt is not crystalline, double deprotonation is performed in pentane with a stoichiometric quantity (2.0 equiv) of $TMSCH_2Li$ (weighed for accurate stoichiometry control). The dilithio salt $Me_2Si(OHF)(CpR^*)Li_2$ (**2**) is soluble in pentane and can be used without further purification. Transmetalation of **2** with a stoichiometric quantity of anhydrous lanthanide trichloride was examined in a variety of ethereal solvents (Et_2O, THF, DME, $^iPr_2O$, or furan) for the synthesis of the $Me_2Si(OHF)(CpR^*)YCl_2Li(ether)_2$ prototypes. In all cases, the reaction is very sluggish and requires up to 3 days to reach completion at room temperature. The ratios of the two product diastereomers were assayed by ^{1}H NMR spectroscopy using the Cp proton signals as probes and vary somewhat, depending on the ethereal solvent employed. The crystallinity of the products also depends on the solvent, and there are qualitative correlations between the crystallinity of the products and the diastereomeric purity of the complexes formed, with results summarized in Table 2.

(17) (a) Hoye, T.; Renner, M. K. *J. Org. Chem.* **1996**, *61*, 2056−2064. (b) Hoye, T.; Renner, M. K. *J. Org. Chem.* **1996**, *61*, 8489−8495. (c) Dale, J. A.; Dull, D. L.; Mosher, H. S. *J. Org. Chem.* **1969**, *9*, 2543−2549.

(18) $[\alpha]^{20}_D$ = −20.0° for (*R*)-(−)-2-methylpyrrolidine and $[\alpha]^{20}_D$ = −24.3° for (*R*)-(−)-2,4,4-trimethylpyrrolidine; see: (a) Ringdahl, B.; Pereira, W. E., Jr.; Craig, J. C. *Tetrahedron* **1981**, *37*, 1659−1662. (b) Reference 17a. (c) Craig, J. C.; Roy, S. K. *Tetrahedron* **1965**, *21*, 401−406. (d) Ripperger, H.; Schreiber, K. *Tetrahedron* **1965**, *21*, 407−412.

(19) (a) Burk, M. J.; Pizzano, A.; Martin, J. A.; Liable-Sands, L. M.; Rheingold, A. L. *Organometallics* **2000**, *19*, 250−260.

(20) Cromer, D. T.; Waber, J. T. *International Tables for X-ray Crystallography*; Kynoch Press: Birmingham, England, 1974; Vol. IV.

(21) Sheldrick, G. M. SHELXS-97; University of Göttingen, Göttingen, Germany, 1997.

(22) Sheldrick, G. M. SHELXL-97; University of Göttingen, Göttingen, Germany, 1997.

(23) Full-matrix least-squares refinement on F^2: wR2 = $\{\sum(w(F_o^2 - F_c^2)^2)/[\sum(w(F_o^2)^2\}^{1/2}$.

Table 2. Effect of Synthesis Solvent on the Diastereomeric Purity and Crystallinity of $Me_2Si(OHF)(CpR^*)YCl_2(ether)_2$ (3b)

ethereal solvent	diastereomeric ratio	product form
Et_2O	70:30	oily
THF	80:20	semisolid
DME	90:10	crystalline
$^iPr_2O$	60:40	oily
furan	70:30	oily

In the $Me_2Si(Cp'')(CpR^*)LnCl_2Li(ether)_2$ systems, the thermodynamically less stable diastereomers (kinetic products) can be isolated in pure form by careful control of the reaction conditions (e.g., temperature, solvent, etc.).[11] However, in the present OHF systems, the predominant diastereomer formed is of the same configuration under all reaction conditions investigated. DME adducts exhibit a marked decrease in solubility and are prepared by exchanging coordinated ether at room temperature via three cycles of DME condensation−stirring−evacuation. Following this process, isolating these $Me_2Si(OHF)(CpR^*)LnCl_2Li(DME)_2$ complexes is straightforward. After isolation of these adducts, ^{1}H NMR spectra still reveal the presence of two diastereomers, and the ratios of these signals remain invariant during the ether exchange process.[24]

Several attempts were made to purify the diastereomeric mixtures of the ether and DME adducts by fractional crystallization. For the ether adducts, the solubility of the complex proved to be too great to obtain a crystalline solid by recrystallization from diethyl ether, as was employed for purification of the Cp″ analogues.[11] In less polar solvents such as pentane, ethereal adducts are unstable toward salt elimination at room temperature, and a dimeric chloride complex is isolated (eq 1). A low-temperature single-crystal X-ray

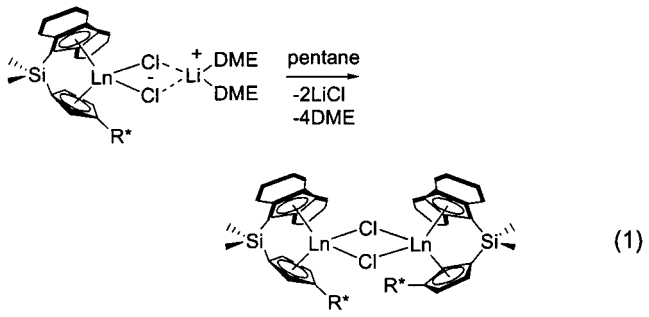

(1)

structure investigation was carried out on a typical and rather marginal quality crystal of the dimeric yttrium chloride complex (grown from a concentrated pentane solution). The two OHF rings are located on the same side of the complex with respect to the $Y-Cl_2-Y$ plane, and the structure has crystallographically imposed C_2 symmetry. The facial chirality with regard to the orientation of the menthyl−Cp ring was established as the *S* configuration from the data. There is precedent for this type of fluorenyl ring disposition in an organolanthanide (μ-Cl)$_2$ dimer.[16a] Because of these complications, purification of the ether adducts was not investigated further.

The as-prepared DME adducts exhibit the highest crystallinity and greatest diastereopurity of the products obtained in this study and can be recrystallized from hot DME (cooling from reflux to room temperature). Although these complexes can be isolated in a highly crystalline form, no effective additional diastereoenrichment was obtained beyond the initial ratio (ca. 90:10). It was found that all complexes recovered from the recrystallization mother liquor evidence slight diastereoenrichment (90:10 → 97:3 by ^{1}H NMR); however, this product represents only 10−20% of the initial amount and is still not completely diastereomerically pure. At this point, additional separation of the 90:10 diastereomeric mixture was not attempted, and the material was used in the next synthetic step without further purification. Analogous dichloride complexes of Sm and Lu were also prepared via routes similar to that for $Me_2Si(OHF)(CpR^*)LnCl_2Li(DME)_2$ adducts (Ln = Sm, **3a**; Ln = Y, **3b**; Ln = Lu, **3c**) and the diastereomeric ratios were ca. 90:10 in all cases.

Conversion of the above dichloro−DME complexes to the corresponding amido hydroamination and hydrophosphination catalyst precursors was effected according to methods developed for other lanthanocenes.[11] The reaction between diastereomerically enriched **3b** and 1.0 equiv of $KN(TMS)_2$ in toluene affords $Me_2Si(OHF)(CpR^*)YN(TMS)_2$ (**4b**) in quantitative yield by ^{1}H NMR. At room temperature, the reaction proceeds within several hours with essentially complete retention of diastereomeric purity. Thus, the ratio of the two diastereomers in the crude amido complex is also ca. 90:10, as was observed for the starting chloro complex. The amido complexes exhibit appreciable thermal stability and can be extracted with boiling hexane. A single recrystallization from hot hexane is sufficient to obtain a single configuration of the amido complex in complete diastereopurity, as assayed by ^{1}H NMR. The dichloro−DME complexes of Sm and Lu were converted into the corresponding amido complexes by procedures similar to that used for the Y analogue and were isolated diastereomerically pure in 69% (**4a**) and 72% (**4c**) yields, respectively.[24,25]

Molecular Structure of the Precatalyst (*S*)-$Me_2Si(OHF)(CpR^*)YN(TMS)_2$ (4b). Single crystals of **4b** suitable for X-ray diffraction were grown from a concentrated hot hexane solution, and the molecular structure is shown in Figure 1, with pertinent bond lengths and angles compiled in Table 3. The structure can be compared to those of the analogous $Me_2Si(Cp'')(CpR^*)LnN(TMS)_2$ complexes,[11] in which the absolute configurations were assigned on the basis of the diffraction data. Similarly, the present structure is assigned the *S* configuration. The ring centroid−Ln−ring centroid angle in the OHF complex is nearly identical with that in analogous Cp″ complexes, with the present complex having an angle of 122.3°, versus 122.1° for (*R*)-$Me_2Si(Cp'')(CpR^*)YN(TMS)_2$ (R* = (−)-menthyl).[11] The Y−ring carbon bond distances for the two types of π ligands in **4b** are nearly equivalent, with Y−C(CpR*) = 2.596(2)−2.785(2) Å versus Y−C(OHF) = 2.598(2)−2.760(2) Å. Similar distances are observed in the analogous Cp″ complexes, with representative distances Y−C(CpR*) =

(24) The dichloro complexes and amido precatalysts were characterized by multinuclear NMR and elemental analysis, as detailed in the Experimental Section.

(25) Conversion of the DME adducts into the corresponding hydrocarbyl complexes with $LiCH(TMS)_2$ or $KCH(TMS)_2$ has not yet been accomplished with acceptable diastereoselectivity.

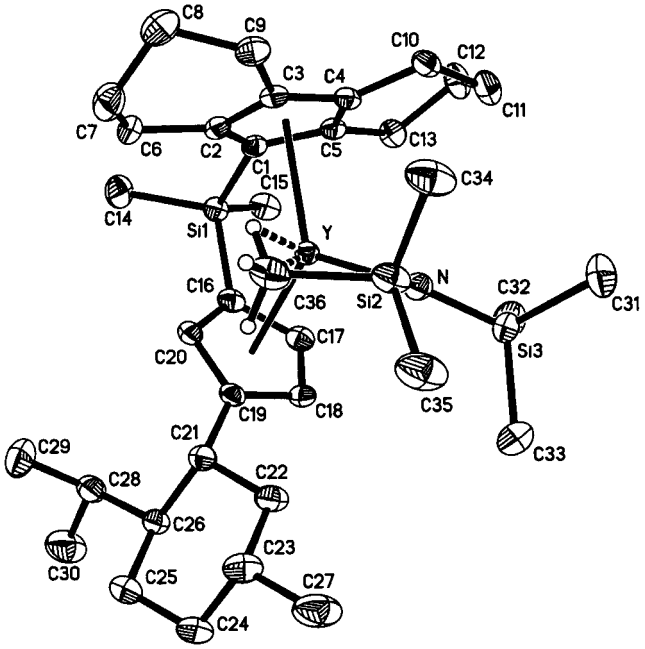

Figure 1. Molecular structure of (*S*)-$Me_2Si(OHF)(CpR^*)YN(TMS)_2$ (**4b**; R* = (−)-menthyl). Thermal ellipsoids are drawn at the 50% probability level.

Table 3. Selected Bond Distances (Å) and Angles (deg) for $Me_2Si(OHF)(CpR^*)YN(TMS)_2$ (4b)

Bond Distances			
Y−N1	2.2541(14)	Y−C36	2.8182(19)
N−Si2	1.7026(16)	Si2−C36	1.911(2)
N−Si3	1.7104(16)	Si2−C35	1.864(2)
Y−C1	2.5977(17)	Y−C16	2.5957(17)
Y−C2	2.6529(17)	Y−C17	2.6080(18)
Y−C3	2.7600(17)	Y−C18	2.7329(17)
Y−C4	2.7234(17)	Y−C19	2.7848(16)
Y−C5	2.6130(16)	Y−C20	2.6403(16)
Si1−C1	1.8679(18)	Si1−C16	1.8637(18)

Bond Angles			
Y−N−Si2	103.29(7)	N−Si2−C36	106.00(8)
Y−N−Si3	131.85(8)	N−Si2−C35	116.74(10)
Si2−N−Si3	123.99(9)	C1−Si1−C16	98.77(7)
N−Y−C16	139.55(5)	N−Y−C1	141.04(5)
Cp_{cent}-Y−OHF_{cent}	122.3(9)		

2.590(9)−2.79(1) Å and Y−C(Cp″) = 2.59(1)−2.70(1) Å.[11] The two TMS groups in the amide ligand of **4b** are inequivalent, as shown in Figure 1, and the corresponding resonances in the ^{1}H NMR are separated by 0.06 ppm. The Y−N−Si2 angle is more acute than the Y−N−Si3 angle by 28.56°, and the Si2−C36 bond is tilted toward the Y center. The Si2−C36 distance is 1.911(2) Å, which is the longest of the six Si−C bonds in the TMS groups of the molecule (the average of the other five C−Si bonds is 1.872(2) Å). This distortion indicates a well-documented type of agostic interaction between the Y and the Si2−C36−H36 functionality.[26,27] The Si3−Y distance is 3.626(2) Å, which is 0.504 Å longer than the Si2−Y distance of 3.112(2) Å. The N−Si2 and N−Si3 bond lengths are similar, suggesting little interaction between Y and either of the N−Si bonds.

(26) General references on agostic interactions: (a) Grubbs, R. H.; Coates, G. W. *Acc. Chem. Res.* **1996**, *29*, 85−93. (b) Brookhart, M.; Green, M. L. H.; Wong, L.-L. *Prog. Inorg. Chem.* **1988**, *36*, 1−124.

(27) Organolanthanide agostic interactions: (a) Klooster, W. T.; Brammer, L.; Schaverien, C. J.; Budzelaar, P. H. M. *J. Am. Chem. Soc.* **1999**, *121*, 1381−1382. (b) Reference 6b. (c) Stern, D.; Sabat, M.; Marks, T. J. *J. Am. Chem. Soc.* **1990**, *112*, 9558−9575. (d) den Haan, K. H.; de Boer, J. L.; Teuben, J. H.; Spek, A. L.; Krojc-Prodic, B.; Hays, G. R.; Huls, R. *Organometallics* **1986**, *5*, 1726−1733.

Scheme 2. Proposed Catalytic Cycle for Cyclization of Amino- and Phosphinoalkenes by $Me_2Si(OHF)(CpR^*)LnN(TMS)_2$ Precatalysts

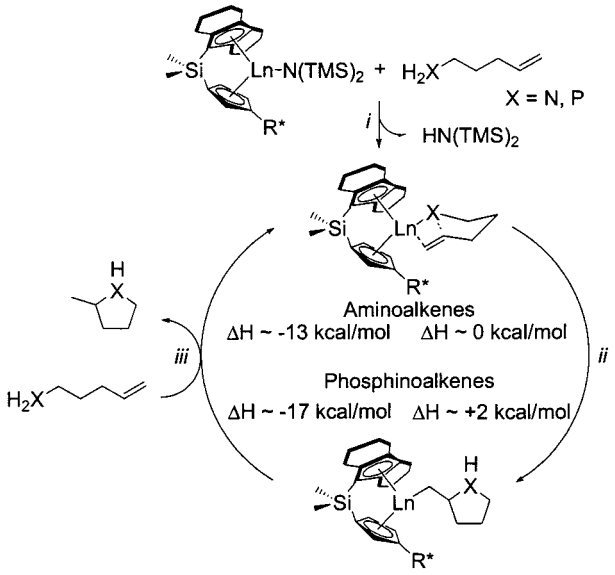

Catalyst Generation and Stereochemical Integrity. The reaction of the present organolanthanide precatalysts with olefinic amine and phosphine substrates is envisioned to proceed through a reasonably well-established catalytic cycle (Scheme 2);[8,9] after initial protonolysis of the precatalyst Ln−N bond (step *i*), the first (turnover-limiting) step of the cycle (step *ii*) is insertion of the C=C double bond into the Ln−heteroatom bond, followed by more rapid protonolysis (step *iii*) of the resulting Ln−C bond to generate the heterocyclic product and a new Ln−heteroatom bond. The catalyst activation process does not, however, proceed as rapidly as expected. Previous studies with other lanthanocene amido precatalysts and amine substrates found the protonolytic generation of $HN(TMS)_2$ to be essentially instantaneous and quantitative, even at −78 °C.[8] For the present more sterically encumbered OHF precatalyst, step *i* with aminoalkenes is not always instantaneous and is instead dependent on both the substrate concentration and also the lanthanide ion size. For example, the reaction of ∼4−5 equiv of *n*-propylamine with **4b** at millimolar concentrations in C_6D_6 requires a period of more than 1.0 h for complete Y−$N(TMS)_2$ protonolysis, whereas the same protonolysis with ∼200 equiv of *n*-propylamine occurs within minutes at room temperature. Therefore, when the kinetics of aminoalkene cyclizations were monitored in this study, either a comparatively large (>50:1) substrate:catalyst ratio was employed or the kinetics were not monitored until after the initial activation period was complete, as judged by ^{1}H NMR. In some cases with complexes of smaller lanthanide ions, this slow activation process precluded accurate kinetic measurements entirely, because the concentration of active catalyst slowly increased throughout the course of the reaction.

For phosphinoalkenes, step *i* of the catalytic cycle is exceedingly sluggish, even at elevated temperatures. This is not entirely surprising, given the slow rate of protonolytic reaction of alkylphosphines with achiral $Cp'_2LnCH(TMS)_2$ precatalysts.[9] To activate the present precatalysts for subsequent reactions with phosphine

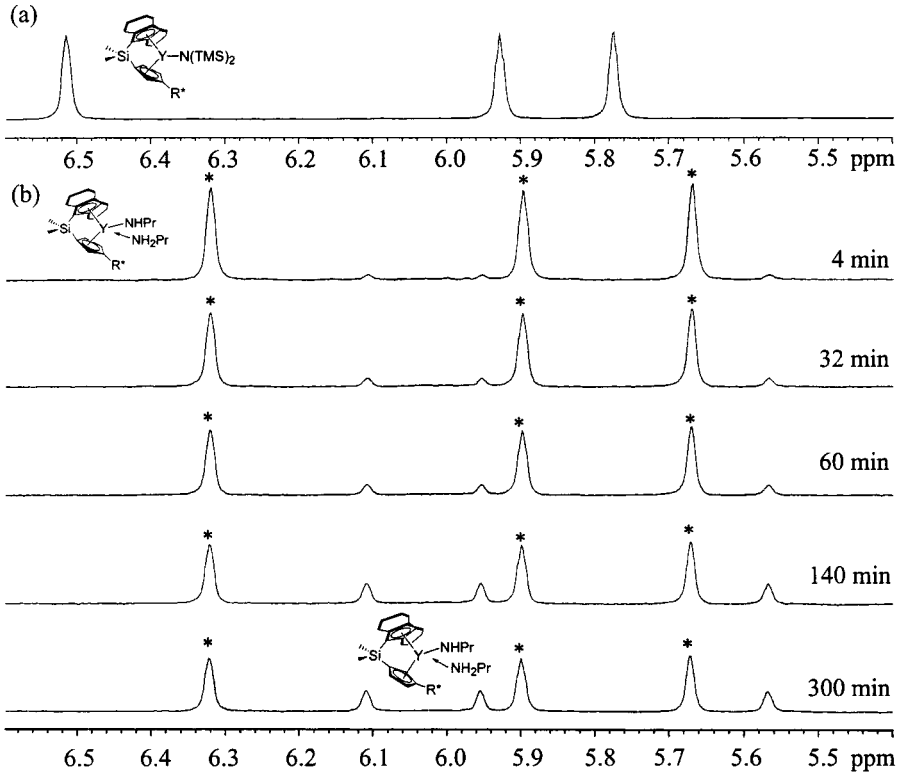

Figure 2. ^{1}H NMR spectra of the Cp region of the precatalyst (*S*)-$Me_2Si(OHF)(CpR^*)YN(TMS)_2$ (**4b**) + ~200 equiv of *n*-propylamine in C_6D_6 at 23 °C: (a) precatalyst (*S*)-$Me_2Si(OHF)(CpR^*)YN(TMS)_2$, before the addition of *n*-propylamine; (b) relaxation of (*S*)-$Me_2Si(OHF)(CpR^*)Y(NHPr)(NH_2Pr)$ to an (*R,S*)-$Me_2Si(OHF)(CpR^*)Y(NHPr)(NH_2Pr)$ equilibrium mixture. The asterisks indicate the initial resonances of the *S* isomer, and the unlabeled peaks represent the formation of the *R* isomer.

Scheme 3. Proposed Mechanism for the Epimerization of (*S*)-$Me_2Si(OHF)(CpR^*)Ln(NHR)(NH_2R)$ Catalysts

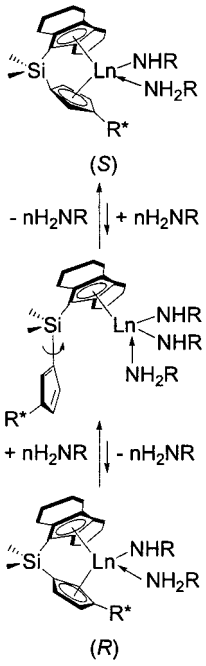

substrates, it was found that addition of ~10 equiv of *n*-propylamine (subsequently removed in vacuo, vide infra) effected rapid and complete protonolytic elimination of $HN(TMS)_2$ to yield an active catalyst. Formation of a hydride precatalyst (an effective solution to this problem with $Cp'_2LnCH(TMS)_2$ catalysts)[9] is not possible in this instance, because $LnCH(TMS)_2$ derivatives were not available and because Ln−N linkages do not typically undergo efficient hydrogenolysis.[28]

In addition to the aforementioned sluggish activation reaction, an epimerization process is also detected in the presence of amines by monitoring the Cp resonances in the ^{1}H NMR spectrum (e.g., Figure 2). The amine−amido complex, generated from the protonolytic reaction of excess amines with precatalyst, undergoes epimerization to degrade the diastereomeric purity of the catalyst. Thus, a 70:30 *S*:*R* epimer ratio is established in the presence of an ~200-fold excess of *n*-propylamine within ~3 h at 23 °C. Although the mechanism of the epimerization is not unambiguously defined, it probably proceeds through a CpR* protonolytic pathway because of the coordinative unsaturation of the metal center (Scheme 3). Such an epimerization process was also identified in the case of $Me_2Si(Cp'')(CpR^*)Ln$ catalysts, and similarly the *S* isomer of $Me_2Si(Cp'')(CpR^*)Ln(NHPr)(NH_2Pr)$ is preferred (>95:5) when R* = (−)-menthyl (eq 2).[11] The equilibrium ratios are typically

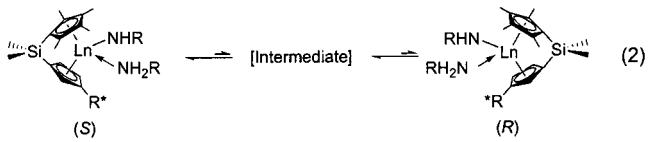

80:20 or greater in these $Me_2Si(Cp'')(CpR^*)Ln$ systems, and the configuration of the major epimer varies de-

(28) For a description of Cp'_2Ln- complexes susceptible to hydrogenolysis, see ref 2d, pp 932−940.

Table 4. Rate, Product Enantiomeric Excess, and Absolute Configuration Data for the Catalytic Hydroamination/Cyclization of Aminoalkenes Mediated by Chiral OHF Organolanthanide Precatalysts[a]

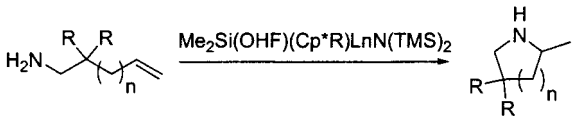

5: n = 1, R = H
7: n = 1, R = CH_3
9: n = 2, R = H
11: n = 2, R = CH_3

6: n = 1, R = H
8: n = 1, R = CH_3
10: n = 2, R = H
12: n = 2, R = CH_3

entry	substrate	precatalyst (Ln center)	N_t (h^{-1})	temp (°C)	% enantiomeric excess (sign)[b]
1	**5**	**4a** (Sm)	2.6	25	46 (+)
2	**5**	**4a** (Sm)	28.4	60	37 (+)
3	**5**	**4b** (Y)	2.9	60	5 (+)
4	**5**	**4c** (Lu)	*c*	60	16 (−)
5	**7**	**4a** (Sm)	33.4	25	32 (+)
6	**7**	**4b** (Y)	*c*	25	17 (+)
7	**7**	**4c** (Lu)	*c*	25	1.5 (+)
8	**9**	**4a** (Sm)	6.6	60	10 (+)
9	**9**	**4b** (Y)	3.6	60	3.2 (+)
10	**11**	**4a** (Sm)	0.6	25	41 (+)
11	**11**	**4a** (Sm)	1.8	40	41 (+)
12	**11**	**4a** (Sm)	89.4	60	43 (+)
13	**11**	**4b** (Y)	2.1	25	67 (+)
14	**11**	**4b** (Y)	86	60	54 (+)
15	**11**	**4c** (Lu)	*c*	60	15 (+)
16	**5**	**4d**[d] (Sm)	33	25	62(+)
17	**7**	**4d**[d] (Sm)	84	25	53(+)
18	**11**	**4d**[d] (Sm)	2	25	15 (−)

[a] Conditions: [substrate]/[catalyst], (30−150):1, C_6D_6, complete consumption of substrate by ^{1}H NMR, N_t calculated from 2 half-lives. The configuration was determined by polarimetry. [b] A + optical rotation correlates to the *S* configuration for these pyrrolidines and piperidines.[18] [c] Turnover frequency not measured because of slow rate of precatalyst activation. [d] Catalyst **4d** = (*S*)-$Me_2Si(Cp'')(CpR^*)SmN(TMS)_2$, R* = (−)-menthyl, data from ref 13.

pending on the chiral auxiliary R*; the *S* epimer is favored when R* = (−)-menthyl, (−)-phenylmenthyl, whereas the *R* epimer is favored when R* = (+)-neomenthyl. In fact, because of this rapid epimerization, the selectivities in hydroamination/cyclizations mediated by these catalysts were found to be insensitive to the initial stereochemical configuration of the precatalyst.[13]

Catalytic Hydroamination/Cyclization. Despite the aforementioned complexities, the present OHF-based catalysts are effective for the asymmetric hydroamination/cyclization of a variety of aminoalkenes (Table 4). The reaction kinetics are found to be zero-order in substrate concentration over at least 3 half-lives for pentenyl substrates **5** and **7** and first-order in catalyst concentration, supporting the same mechanistic scenario observed with other organolanthanide-catalyzed cyclizations (eq 3). Turnover frequencies are

$$v = k[\text{substrate}]^0[\text{catalyst}]^1 \qquad (3)$$

significantly greater than those observed with Cp'_2Ln ligand systems and slightly lower than those observed with homologous chiral $Me_2Si(Cp'')(CpR^*)Ln$ systems (Table 4; entries 1 and 16, entries 5 and 17).[13] The enantioselectivities of the reactions were assayed by GC analysis of the Mosher amide derivatives of the products.[17] In the case of pentenyl substrates **5** and **7**, the results in Table 4 show modest selectivity (ee values up to 46%) at best, slightly less than that observed in the $Me_2Si(Cp'')(CpR^*)Ln$ systems.[13] *gem*-Dimethyl substitution on the substrate carbon backbone enhances the cyclization rate as expected;[8,29] however, the enantioselectivity is slightly diminished. Turnover frequencies for both substrates **5** and **7** follow the same trend with lanthanide ionic radius that was previously observed for aminoalkene cyclizations,[7] namely $Sm^{3+} > Y^{3+} > Lu^{3+}$.[30] Cyclizations **5** → **6** and **7** → **8** show a *decrease* in selectivity with decreasing ionic radius, analogous to the $Sm^{3+}-Y^{3+}-Lu^{3+}$ trend observed with $Me_2Si(Cp'')(CpR^*)Ln$ catalysts,[13] including a change in product absolute configuration for the smallest Lu^{3+} catalyst (Table 4, entry 4).

Hexenylamine cyclizations of **9** → **10** exhibit poor enantioselectivity (≤10%); however, the **11** → **12** cyclization displays substantially greater selectivity, with the intermediate ionic radius Y^{3+} exhibiting the highest ee of 67% (Table 4, entry 13). *gem*-Dimethyl substitution on the substrate carbon backbone must play an integral part in influencing enantioselection, and the ee's with the present OHF ligand system are significantly greater than those previously observed for hexenyl substrates with other chiral organolanthanide catalysts (Table 4, entry 18).[13] In the (*S*)-$Me_2Si(Cp'')(CpR^*)Ln$ systems, four different chairlike cyclic transition states were proposed, with olefin activation/insertion occurring along one of two different idealized trajectories: either "frontally" along the ring centroid−Ln−ring centroid bisector (eqs 4 and 5) or "laterally" approximately along the perpendicular to the ring centroid−Ln−ring centroid plane and presumably distal to the R* chiral blocking group (eqs 6 and 7). Selectivity in the Cp′/Cp″ system (highest with pentenyl substrates) was explained primarily by unfavorable nonbonded interactions between axial C−H groups and the cyclopentadienyl ligands in configurations analogous to those in eqs 5 and 7. The enantioselection in the OHF system can also be explained with the analogous model by correlating the *S* product with an excess of *S* catalyst epimer. Thus, the observed predominant *S* configuration of the product can be rationalized through either a frontal (eq 4) or lateral (eq 6) olefin approach. The *R* product configuration, which in theory could also be obtained via either pathway, requires unfavorable nonbonded interactions between the *gem*-dimethyl groups and the OHF ligand (eq 5) or bulky R* group (eq 7) and, therefore, is not the predominant product. This enhanced stereoselection versus the $Me_2Si(Cp'')(CpR^*)Ln$ systems must arise not only from the steric demands of the ancillary ligands but also from the steric encumbrance of the substrate methyl groups, since selectivity enhancements for the cyclization of the more sterically demanding substrate **11** → **12** are substantially higher than those observed for the cyclization **9** → **10**. On the other hand, the decreased ee values in the cyclization of **5** → **6** and **7** → **8** compared to those from the $Me_2Si(Cp'')(CpR^*)Ln$ systems could be attributed to the lower catalyst epimer equilibrium ratio (70:30 vs >95:5).

(29) Kirby, A. J. *Adv. Phys. Org. Chem.* **1980**, *17*, 183−278.
(30) Sm^{3+} = 1.079 Å, Y^{3+} = 1.019 Å, Lu^{3+} = 0.977 Å: Shannon, R. D. *Acta Crystallogr.* **1976**, *A32*, 751−760.

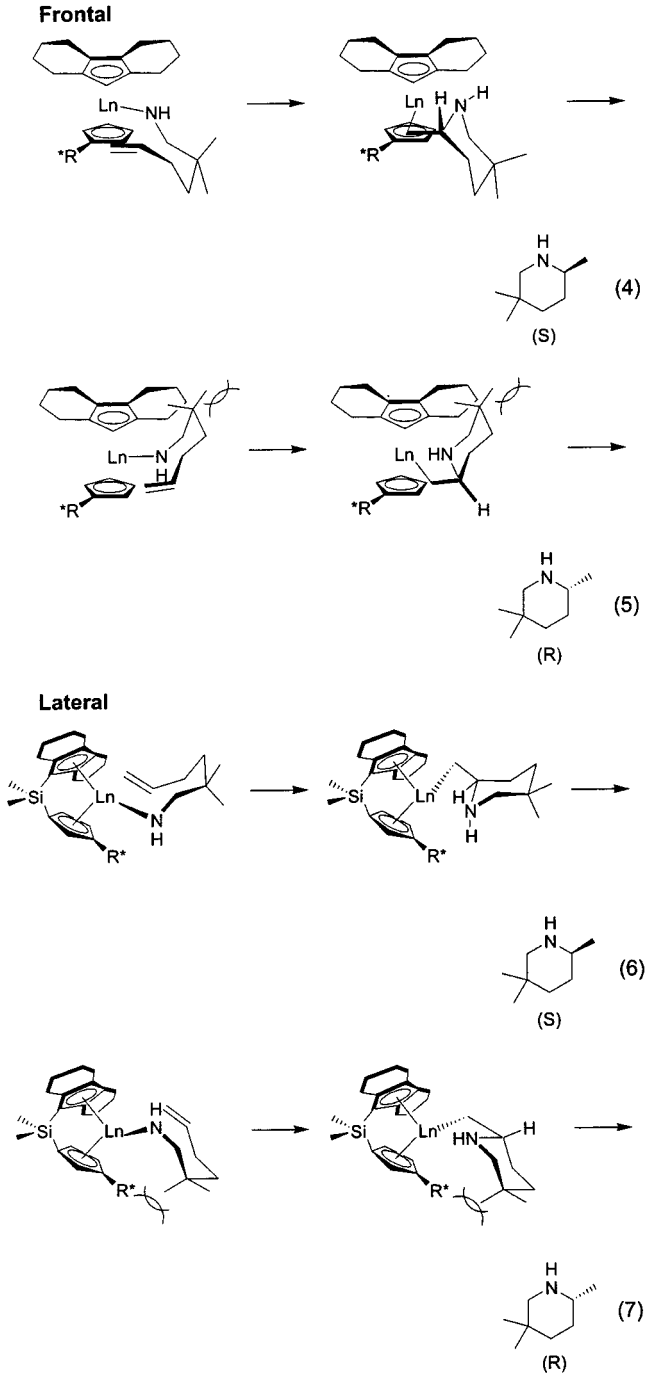

With all four aminoalkenes investigated, changes in selectivity are small when the reactions are carried out at elevated temperatures (Table 4, entries 10−12), which is advantageous in the cases of some of the more sluggish cyclizations. Turnover frequencies for hexenylamines are again slightly lower than those observed with $Me_2Si(Cp'')(CpR^*)Ln$ systems (entries 10 and 18). Interestingly, rather than displaying strictly zero-order kinetics in [substrate], cyclohydroamination processes with hexenyl substrates **9** and **11** actually evidence a slight *increase* in conversion rates with time. This may indicate that the heterocyclic product cannot compete with the primary amine substrate for coordination to the metal center, and therefore as more substrate is consumed, there is an increase in turnover frequency. The reason for this phenomenon was not investigated in detail.

Table 5. Diastereomeric Excess Data for the Catalytic Hydrophosphination/Cyclization of Phosphinoalkenes Mediated by Chiral Organolanthanide OHF Precatalysts[a]

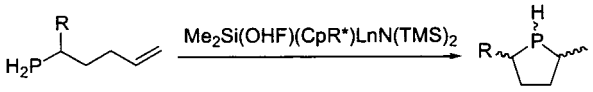

13: R = H
15: R = CH_3

14: R = H
16: R = CH_3

entry	substrate	precatalyst (Ln center)	% cis + trans[b]	% de (temp, °C)
1	**13**	**4a** (Sm)	81	88 (25)
2	**13**	**4b** (Y)	75	78 (25)
3	**13**	**4c** (Lu)	78	83 (25)
4	**15**	**4a** (Sm)	82	96 (0)
5	**15**	**4a** (Sm)	86	91 (25)
6	**15**	**4b** (Y)	68	77 (25)
7	**15**	**4c** (Lu)	72	90 (25)

[a] Conditions: [substrate]/[catalyst], (30−150):1, C_6D_6 or C_7D_8, catalyst initiated with ∼10 equiv of *n*-propylamine, monitored to complete consumption of substrate by ^1H and ^{31}P NMR. [b] Percent of product not tabulated is a phosphorinane side product formed through a noncatalytic route[9a] and a small amount of a third phospholane.[34]

Catalytic Hydrophosphination/Cyclization. The organolanthanide OHF-based catalysts are highly effective for diastereoselective hydrophosphination/cyclizations (Table 5). After the precatalysts were activated with *n*-propylamine to effect rapid $HN(TMS)_2$ elimination, followed by removal of both amines and solvent in vacuo, the phosphine substrate (as a ∼1 M solution in C_6D_6 or C_7D_8) was added and the ensuing cyclization monitored by ^{31}P NMR. One drawback to this procedure is that the $HN(TMS)_2$ generated in catalyst initiation is also removed; thus, there is no convenient way to quantitatively assay the extent of activation. Qualitatively, turnover is most rapid with Sm^{3+} and slows with decreasing lanthanide ionic radius, as was observed above for aminoalkenes. The ^{31}P NMR assayed product ratio is conversion-independent, indicating that selectivity is also conversion-independent. The reaction kinetics are zero-order in substrate concentration, with some evidence for competitive inhibition by product at higher conversions.[9a] The reaction rates are also first-order in catalyst, arguing for the same mechanism as has been previously documented for achiral hydrophosphination/cyclization by organolanthanide catalysts.[9]

Because inversion at phosphorus is slow,[31] cyclization of *ω*-phosphinoalkenes generates two different stereocenters, and therefore the cyclization **13** → **14** can in principle produce two diastereomers and four enantiomers (eq 8). The diastereomers have well-separated chemical shifts in the ^{31}P NMR; hence, the relative stereochemistries can be assigned and the diastereoselectivity of the reactions readily assayed.[32] All of the OHF catalysts screened display high selectivity for formation of *trans*-**14** (Table 5). Interestingly, isolated phospholane product **14** undergoes a slow isomerization (over a period of several weeks) to a final ratio of ∼2:1

(31) The barrier to inversion at trigonal phosphorus is typically ∼35 kcal/mol: (a) Quin, L. D.; Hughes, A. N. *The Chemistry of Organophosphorus Compounds*; Hartley, F. R., Ed.; Wiley: Chichester, U.K., 1990; Vol. 1, pp 295−394. (b) Baechler, R. D.; Mislow, K. *J. Am. Chem. Soc.* **1970**, *92*, 3090−3093. (c) Rauk, A.; Allen, L. C.; Mislow, K. *Angew. Chem., Int. Ed. Engl.* **1970**, *9*, 400−414.

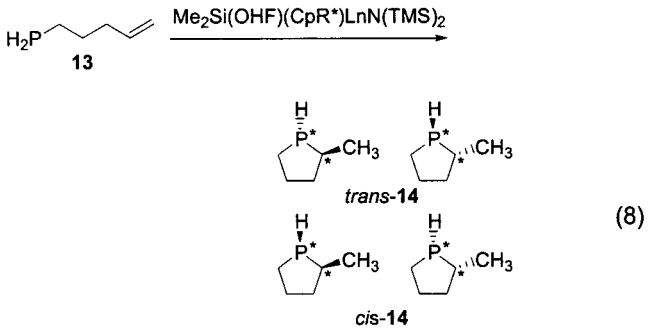

(8)

cis:trans, the same ratio observed with achiral Cp'_2-$LnCH(TMS)_2$ catalysts.[33] If the catalyst and phospholane are not separated after completion of the cyclization, the phospholane undergoes complete isomerization to the same ~2:1 final ratio within 24 h. However, this isomerization does not occur at a significant rate until all substrate has been consumed. Presumably the catalyst can deprotonate and reprotonate the phospholane, leading to the observed isomerization (eq 9).

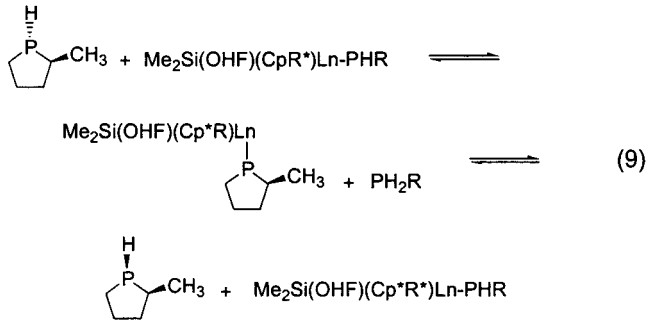

(9)

The cyclization **15** → **16** can in principle yield four isomers, two of which are enantiomorphous (eq 10).[34]

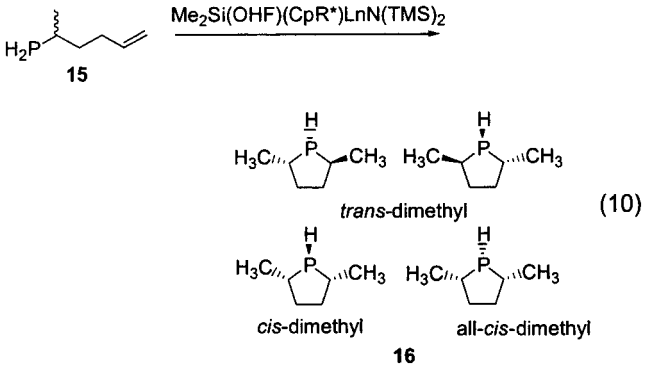

(10)

However, in this case, diastereoselectivity of the OHF catalysts is particularly impressive for the **15** → **16** cyclization (Table 5). Diastereoselectivities as high as 96% are observed for *trans*-**16**, which is a precursor to ligands having many applications in asymmetric catalysis.[19,35]

Conclusions

New chiral C_1-symmetric *ansa*-organolanthanide catalysts with the sterically demanding OHF ligand have been synthesized, resolved, and characterized. Activities for enantioselective aminoalkene hydroamination/cyclization have been measured, and ee values as high as 67% have been observed. In comparison to $Me_2Si(Cp'')$-(CpR*)Ln homologues, the present catalysts exhibit greater enantioselectivities only in the case of sterically encumbered substrates. These octahydrofluorenyl-based catalysts also serve as effective precatalysts for the diastereoselective hydrophosphination of phosphinoalkenes, and de values as high as 96% have been achieved.

Acknowledgment. Financial support by the NSF (Grant No. CHE-0078998) is gratefully acknowledged. We thank Dr. V. Arredondo for helpful discussions.

Supporting Information Available: X-ray crystallographic data, in CIF format, for **4b.** This material is available free of charge via the Internet at http://pubs.acs.org.

OM0104013

(32) For phospholane **14**, the relative conformations of the diastereomers can be assigned by NOESY spectroscopy[9a] or by coupling constant arguments: (a) Langhans, K. P.; Stelzer, O. *Z. Naturforsch.* **1990**, *45b*, 203−211. (b) Couret, C.; Escudie, J.; Thaoubane, S. A. *Phosphorus Sulfur Relat. Elem.* **1984**, *20*, 81−86. The trans form of phospholane **16** has been prepared by another route.[19]

(33) Not surprisingly, heating a solution of phospholane **14** increases the rate of isomerization.

(34) Minimal (<5%) formation of the all-cis phospholane is observed, and this minor product is not considered in the calculation of the de's shown in Table 5.

(35) (a) Burk, M. J. *Acc. Chem. Res.* **2000**, *33*, 363−372. (b) Burk, M. J.; Gross, M. F.; Martinez, J. P. *J. Am. Chem. Soc.* **1995**, *117*, 9375−9376. (c) Burk, M. J.; Harper, G. P.; Kalberg, C. S. *J. Am. Chem. Soc.* **1995**, *117*, 4423−4424. (d) Burk, M. J.; Feaster, J. E.; Nugent, W. A.; Harlow, R. L. *J. Am. Chem. Soc.* **1993**, *115*, 10125−10138.